A Cell Capacitor Energy Balancing Control of Modular Multilevel Converter Considering the Unbalanced AC Grid Conditions

Jae-Jung Jung, Shenghui Cui, Sungmin Kim, *Student Member*, *IEEE*, and Seung-Ki Sul, *Fellow*, *IEEE*
School of Electrical & Computer Engineering
Seoul National University
Seoul, Republic of Korea
Email: jaejung.jung@eepel.snu.ac.kr

***Abstract*— This paper presents a control scheme for the regulation of cell capacitor energy balancing of a Modular Multilevel Converter (MMC) for HVDC transmission systems, considering the unbalanced AC grid conditions. It is essential that the MMC balancing control should be valid not only for the balanced normal operations but also for the asymmetrical grid fault conditions. This paper proposes the control scheme that has the ability of seamless mode change between balanced and unbalanced grid condition. Applying the proposed method, the capacitor energy balancing operation is successfully realized with improved dynamic responses. Finally, the simulation results verify the validity of the proposed method.**

Keywords*— *HVDC transmission system, modular multilevel converter (MMC), unbalanced grid fault, single-line-to-ground fault, capacitor energy balancing.

I. INTRODUCTION

Modular Multilevel Converter (MMC) is a promising and appropriate topology for voltage sourced converter (VSC)-based HVDC transmission. Compared to the two- or three-level standard VSCs whose valves include series connected switches, the MMC for VSC-HVDC allows a reduction of the power losses with very low switching frequency, as well as low dv/dt, low harmonics, and modularity, etc. Due to these advantages of the MMC, many researches about it have been conducted in many aspects [1]-[4]. As one of many concerns about the high power transmission system, grid faults occurrence has to be addressed in the case of MMC based HVDC transmission system. Many researches have been mainly focused on MMC modeling, control strategy, and modulation with balanced grid conditions. And some literatures have discussed the dynamic performance of MMC under grid faults [5]-[9]. This paper deals with the balancing of cell capacitor voltage under asymmetrical grid voltage (e.g., single line-to-ground (SLG) fault, which is the dominant fault mode in the practical transmission lines).

Vector current control derived in the *dq* synchronous reference frame (SRF) has been widely used in three-phase AC/DC converter. To deal with unbalanced grid conditions, a dual current control scheme including positive- and negative-sequence current controller based on vector control concept was introduced in [10], and applied to two-level and three-level grid-connected VSCs. This control scheme had been also applied to the control of MMC-based HVDC system in [8]-[9]. When asymmetrical faults occur at the AC system, there would be negative-sequence components in grid voltages. Therefore, using the dual current controller, negative-sequence current components in grid can be eliminated and the three-phase currents could be kept balanced during the asymmetrical faults [10].

This paper is proposing a control strategy of circulating current for balancing the cell capacitor energy in an MMC under balanced and unbalanced grid condition. The proposed balancing controller exploits the negative sequence components in output phase voltages which should be generated inevitably to eliminate the negative-sequence grid currents in the faulty conditions. Therefore, the proposed method can improve the dynamic performances of MMC under the grid fault condition. Besides, the devised method is universally valid under both balanced and unbalanced grid conditions without any mode transition. So, the fault ride-through capability of the MMC-HVDC system can be enhanced by the proposed control schemes. Finally, to investigate the performance of the proposed controllers, the results of time-domain simulation studies are presented.

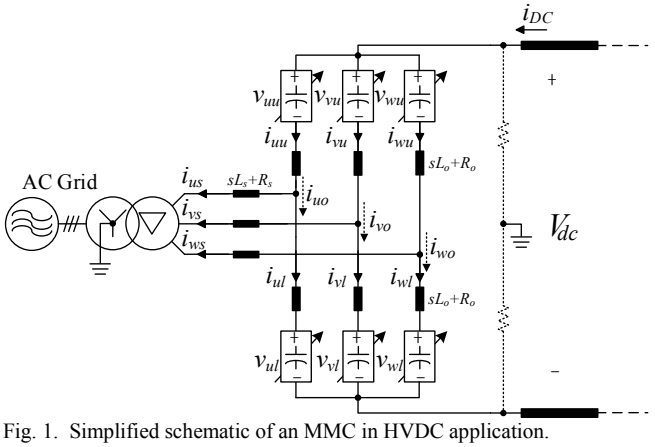

Fig. 1. Simplified schematic of an MMC in HVDC application.

II. CONFIGURATION AND BASIC PRINCIPLE OF THE MMC

The circuit configuration of an MMC in HVDC application is shown as Fig. 1. The three-phase MMC is composed of three legs, and each leg has two arms and two arm inductors. An arm usually consists of numerous half-bridge based sub-module called as cell and the whole arm can be modeled as a high bandwidth controlled voltage source with a capacitor tank. The AC side of MMC is connected to AC grid through a Y/Δ transformer for preventing the zero-sequence phase currents from flowing into the converter. For detailed mathematical description of the model of MMC, the equivalent circuit diagram can be depicted as Fig. 2. In Fig. 2, at first, i_{xu} and i_{xl} are upper and lower arm currents, respectively, and i_{xs} is the grid current, where the notation 'x' denotes a phase among u, v, and w.

In accordance with the conventional definitions [11]-[12], the upper and lower arm, the leg and the circulating current can be defined and deduced as (1)-(4), respectively.

$$i_{xu} = \frac{1}{2} i_{xs} + i_{xo} . \tag{1}$$

$$i_{xl} = -\frac{1}{2} i_{xs} + i_{xo} . \tag{2}$$

$$i_{xo} = \frac{i_{xu} + i_{xl}}{2} = i_{xo,cir} + \frac{1}{3} i_{DC} . \tag{3}$$

$$i_{xo,cir} = i_{xo,cirDC} + i_{xo,cirAC} . \tag{4}$$

The phase voltage can be used to regulate the grid current and the leg current i_{xo} can be regulated by the leg internal voltage. The phase v_{xs} and leg internal voltage v_{xo} are defined as (5) and (6), respectively.

$$v_{xs} = -\frac{1}{2}(v_{xu} - v_{xl}) . \tag{5}$$

$$v_{xo} = \frac{1}{2}\{V_{dc} - (v_{xu} + v_{xl})\} = (R_o + L_o \frac{d}{dt}) i_{xo} . \tag{6}$$

Therefore, the upper and lower arm voltage reference should be (7) and (8) for the desired performances of MMC. Namely, the arm voltage references are sum of independent components for regulating DC bus current, AC output current, and leg current.

$$v_{xu}^* = \frac{V_{dc}^*}{2} - v_{xs}^* - v_{xo}^* . \tag{7}$$

$$v_{xl}^* = \frac{V_{dc}^*}{2} + v_{xs}^* - v_{xo}^* . \tag{8}$$

From the above descriptions, the mechanisms for dealing with the capacitor energy in MMC can be derived. Both DC bus voltage and AC power reference should be determined to keep the total capacitor energy in MMC. And, the controllable component of circulating current has to be used to balance the capacitor energy among six arms. To balance the arm capacitor energy, the power flow into a leg should be considered. Power that flows into upper and lower arms in the same leg are:

$$P_{xu} = v_{xu}^* i_{xu} = (\frac{V_{dc}^*}{2} - v_{xs}^* - v_{xo}^*)(\frac{1}{2} i_{xs} + i_{xo}) . \tag{9}$$

$$P_{xl} = v_{xl}^* i_{xl} = (\frac{V_{dc}^*}{2} + v_{xs}^* - v_{xo}^*)(-\frac{1}{2} i_{xs} + i_{xo}) . \tag{10}$$

Then, the sum and difference of the power between upper and lower arms are:

$$P_x^{\Sigma} = P_{xu} + P_{xl} = V_{dc}^* i_{xo} - v_{xs}^* i_{xs} - 2 v_{xo}^* i_{xo} . \tag{11}$$

$$P_x^{\Delta} = P_{xu} - P_{xl} = \frac{1}{2} V_{dc}^* i_{xs} - 2 v_{xs}^* i_{xo} - v_{xo}^* i_{xs} . \tag{12}$$

And these two equations have to be considered for understanding of the subsequent proposed balancing control. The sum of upper and lower arm energy, E_x^{Σ}, should be controlled by the first power term in right side of (11). Thus, a DC component of leg current, i_{xo}, is injected to regulate E_x^{Σ}. The difference of upper and lower arm energy, E_x^{Δ}, should be counterbalanced by the second term in right side of (12). So, a fundamental frequency component of leg current i_{xo} is injected to control E_x^{Δ}.

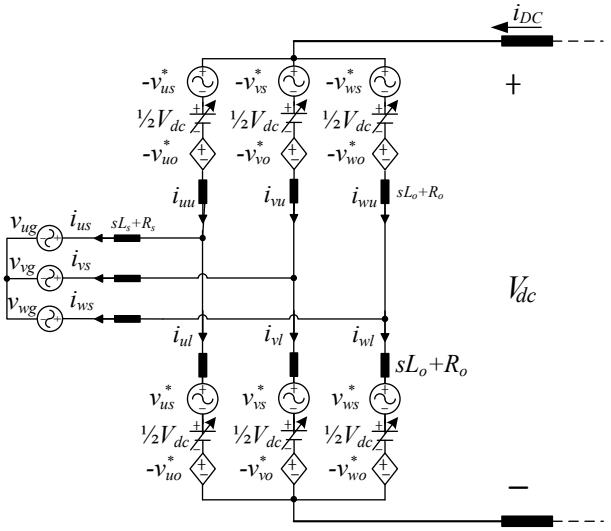

Fig. 2. Equivalent circuit diagram of the MMC.

III. MMC MODELING IN VSC-HVDC TRANSMISSION

In [11], a new modified model of MMC for energy control of cell capacitor has been presented, which divides the MMC model like Fig. 2 into AC grid current model, DC bus current model, and circulating current model. According to the modified model of MMC, the AC grid power control and DC bus voltage control can be decoupled.

The equivalent circuit diagram in Fig. 2 can be divided into three aforementioned simplified equivalent models like Fig. 3. First, for phases x and y, according to KVL, transients of upper and lower arm currents can be derived as (13) and (14).

$$\begin{aligned} &-v_{xs}^* + \frac{1}{2} V_{dc}^* - v_{xo}^* + (L_o \frac{d}{dt} + R_o) i_{xu} + (L_s \frac{d}{dt} + R_s) i_{xs} + v_{xg} \\ &= -v_{ys}^* + \frac{1}{2} V_{dc}^* - v_{yo}^* + (L_o \frac{d}{dt} + R_o) i_{yu} + (L_s \frac{d}{dt} + R_s) i_{ys} + v_{yg} . \end{aligned} \tag{13}$$

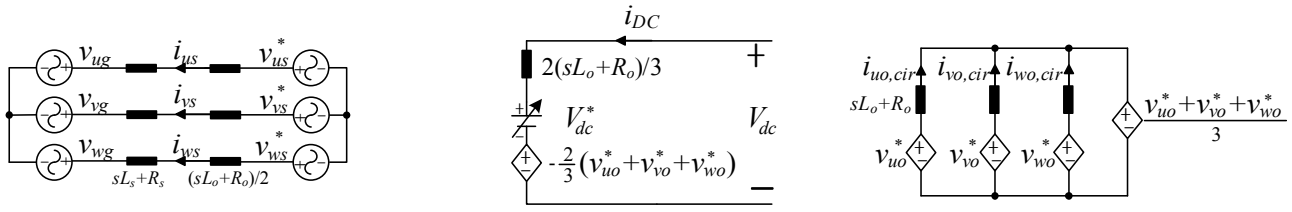

(a) Equivalent model to describe AC grid current. (b) Equivalent model to describe DC bus current. (c) Equivalent model to describe circulating current.

Fig. 3. Simplified equivalent models of AC grid current, DC bus current, and circulating current.

$$\begin{aligned} &v_{xs}^* + \frac{1}{2}V_{dc}^* - v_{xo}^* + (L_o\frac{d}{dt} + R_o)i_{xl} - (L_s\frac{d}{dt} + R_s)i_{xs} - v_{xg} \\ &= v_{ys}^* + \frac{1}{2}V_{dc}^* - v_{yo}^* + (L_o\frac{d}{dt} + R_o)i_{yl} - (L_s\frac{d}{dt} + R_s)i_{ys} - v_{yg}. \end{aligned} \quad (14)$$

Both of (13) and (14) become same one equation of (15) which is basis of AC grid current model, using the definition of leg current in (3) and leg internal voltage in (6).

$$\begin{aligned} &v_{xs}^* - (L_o\frac{d}{dt} + R_o)i_{xs}/2 - (L_s\frac{d}{dt} + R_s)i_{xs} - v_{xg} \\ &= v_{ys}^* - (L_o\frac{d}{dt} + R_o)i_{ys}/2 - (L_s\frac{d}{dt} + R_s)i_{ys} - v_{yg}. \end{aligned} \quad (15)$$

According to (15), a simplified equivalent model to describe the AC grid current can be extracted from Fig. 2, as shown in Fig. 3(a).

Second, the instantaneous DC bus voltage equations of *u*-, *v*-, and *w*-phase by KVL for Fig. 2 can be described as (16).

$$\begin{cases} (-v_{us}^* + \frac{V_{dc}^*}{2} - v_{uo}^*) + (L_o\frac{d}{dt} + R_o)(i_{uu} + i_{ul}) + (v_{us}^* + \frac{V_{dc}^*}{2} - v_{uo}^*) = V_{dc} \\ (-v_{vs}^* + \frac{V_{dc}^*}{2} - v_{vo}^*) + (L_o\frac{d}{dt} + R_o)(i_{vu} + i_{vl}) + (v_{vs}^* + \frac{V_{dc}^*}{2} - v_{vo}^*) = V_{dc} \\ (-v_{ws}^* + \frac{V_{dc}^*}{2} - v_{wo}^*) + (L_o\frac{d}{dt} + R_o)(i_{wu} + i_{wl}) + (v_{ws}^* + \frac{V_{dc}^*}{2} - v_{wo}^*) = V_{dc} \end{cases}. \quad (16)$$

From summation of three equations in (16), DC bus voltage can be deduced as (17).

$$V_{dc}^* + \frac{2}{3}(L_o\frac{d}{dt} + R_o)i_{dc} - \frac{2}{3}(v_{uo}^* + v_{vo}^* + v_{wo}^*) = V_{dc}. \quad (17)$$

According to (17), a simplified equivalent model to describe the DC bus current can be extracted from Fig. 2, as shown in Fig. 3(b).

Meanwhile, (18) can be derived after canceling an *x*-phase equation of (16) and (17) by the DC bus voltage, V_{dc}.

$$(L_o\frac{d}{dt} + R_o)(i_{xo} - \frac{i_{dc}}{3}) = v_{xo}^* - \frac{v_{uo}^* + v_{vo}^* + v_{wo}^*}{3}. \quad (18)$$

A circulating current $i_{xo,cir}$ is defined as the difference between the leg current i_{xo} and a third of the DC bus current that identically flows into each phase:

$$i_{xo,cir} = i_{xo} - \frac{i_{dc}}{3}. \quad (19)$$

Therefore, (20) can be derived from (18) and (19).

$$v_{xo}^* - (L_o\frac{d}{dt} + R_o)i_{xo,cir} = \frac{v_{uo}^* + v_{vo}^* + v_{wo}^*}{3}. \quad (20)$$

And finally, according to (20), a simplified equivalent model to describe the circulating current can be extracted from Fig. 2, as shown in Fig. 3(c).

The average of three phase leg internal voltages (v_{uo}^*, v_{vo}^*, v_{wo}^*) is defined as (21) which is the common mode leg internal voltage $v_{o,com}^*$.

$$v_{o,com}^* = \frac{v_{uo}^* + v_{vo}^* + v_{wo}^*}{3}. \quad (21)$$

As shown in Fig. 3(b), the common mode leg internal voltage $v_{o,com}^*$ affects the real DC bus voltage V_{dc}. Furthermore, $v_{o,com}^*$ of the circulating current model also affects circulating currents as shown in Fig. 3(c). So, in the case of weak DC bus condition in HVDC transmission system, the control dynamics and system performance would significantly depend on the common mode leg internal voltage $v_{o,com}^*$. And, $v_{o,com}^*$ should be controlled as null. Based on above MMC modeling which can completely decouple AC current regulation, DC current regulation, and cell capacitor energy control, Section IV proposes the capacitor energy balancing strategy under balanced and unbalanced grid conditions.

IV. Capacitor Energy Balancing Strategy under Balanced and Unbalanced Grid Conditions

A. Overall Control Scheme in MMC System Considering Unbalanced AC Grid Conditions

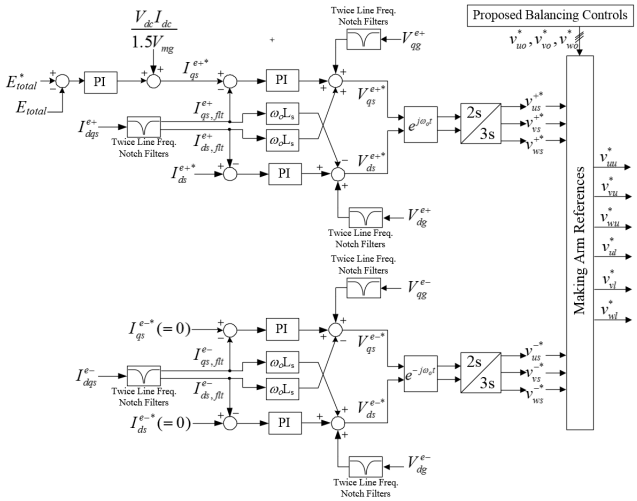

Fig. 4. Control block diagram of the overall control scheme under AC grid unbalanced conditions.

Under the unbalanced grid faults, one of countermeasures to the faults is balancing the grid currents. This can minimize the fault current that may make detrimental effect on the converter. To prevent this fault current effect, the negative-sequence current should be eliminated by setting the references of negative-sequence current controller as zero ($I_{dqs}^{e-*}=0$). The negative-sequence current controller in VSC generates the corresponding negative-sequence output voltage references to suppress the unbalanced currents [8]. Meanwhile, as shown like Fig. 1, Y/Δ transformer connected to AC grid excludes the argument about the zero-sequence component from the converter. Based on above observation, the overall control scheme under unbalanced grid condition can be depicted as shown in in Fig. 4.

This paper proposes a capacitor energy balancing control method that can be applied under unbalanced grid condition as well as balanced grid condition. Especially, this method achieves improved dynamic behavior of the MMC by using the negative-sequence component in output phase voltage of MMC system that is made from negative sequence current controller. For example, if SLG fault occurs at the line side of the MMC, the positive-sequence voltage reduces. In conventional balancing method which only considers positive-sequence component in output phase voltage [8]-[9], the balancing controller should increase the magnitude of circulating current for eliminating the considerable unbalanced capacitor energy. Moreover, a considerable twice fundamental frequency current flows through DC transmission line under SLG fault. However, the proposed method can improve the dynamics by exploiting the negative-sequence output phase voltages from the negative sequence current controller.

B. Balancing of Three Phase Leg Energy

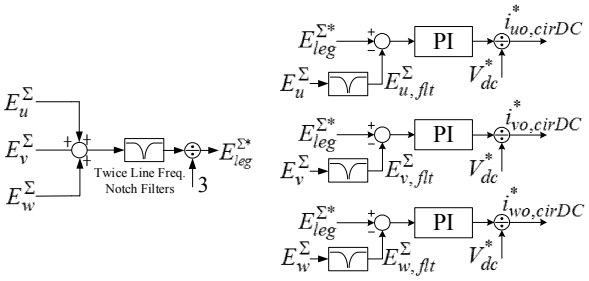

(a) Calculation of leg energy reference. (b) Inter-leg energy balancing controller.

Fig. 5. Control block diagram of the proposed leg capacitor energy balancing controller.

The proposed strategy for the comprehensive cell capacitor energy control in [11] makes the leg capacitor energy balanced and eliminates upper and lower arm capacitor energy difference with excellent performance in view point of both dynamics and stability even under the weak DC grid. The three phase leg energy balancing control is identical to that of proposed method in [11]. The leg capacitor energy balancing controller is shown in Fig. 5. The leg capacitor energy reference is updated as the average capacitor energy of three phase legs at every sampling instant as shown in Fig. 5(a). The philosophy of using the average energy of three legs as the reference is balancing inner-converter leg capacitor energy by only controlling the circulating currents, without affecting the energy flows from AC grid or DC bus into the whole three phase converter. And, the capacitor energy among three legs can be balanced by DC component of circulating currents as shown by the outputs of controllers in Fig. 5(b). Because the leg capacitor energy reference is calculated and updated at every sampling period, it can be valid that the common mode leg internal voltage $v_{o,com}^{*}$ is inherently null, as (22).

$$\sum_{x=u,v,w}(E_{leg}^{\Sigma*}-E_{x,flt}^{\Sigma})=0.\Rightarrow\sum_{x=u,v,w}i_{xo,cirDC}^{*}=0.\Rightarrow\sum_{x=u,v,w}v_{xo,DC}^{*}=0. \quad (22)$$

C. Balancing of Upper and Lower Arm Capacitor Energy under Balanced and Unbalanced Grid Conditions

As with many conventional researches about energy balancing control [11]-[12], the second term in right side of (12) is employed for balancing of upper and lower arm capacitor energy. Thus, the energy difference between upper and lower arms can be eliminated by injecting a fundamental frequency on leg currents or circulating currents. Like the preceding about nullifying the common mode leg internal voltage $v_{o,com}^{*}$, the common mode AC circulating current reference at fundamental frequency should be null as (23).

$$\sum_{x=u,v,w}v_{xo,AC}^{*}=0\ .\ \Rightarrow\sum_{x=u,v,w}i_{xo,cirAC}^{*}=0. \quad (23)$$

Considering the grid fault condition, the output phase voltage reference has the negative sequence components which should be generated inevitably to eliminate the negative grid currents as referred at Fig 4.

First, assuming unbalanced grid condition, the positive- and negative-sequence component of the output phase voltages are defined by (24) and (25), respectively.

$$\begin{cases}v_{us}^{+*}=V_{ms}^{+}\sin(\omega_o t+\phi_v^{+})\\ v_{vs}^{+*}=V_{ms}^{+}\sin(\omega_o t+\phi_v^{+}-2\pi/3)\\ v_{ws}^{+*}=V_{ms}^{+}\sin(\omega_o t+\phi_v^{+}+2\pi/3)\end{cases}. \quad (24)$$

$$\begin{cases}v_{us}^{-*}=V_{ms}^{-}\sin(\omega_o t+\phi_v^{-})\\ v_{vs}^{-*}=V_{ms}^{-}\sin(\omega_o t+\phi_v^{-}+2\pi/3)\\ v_{ws}^{-*}=V_{ms}^{-}\sin(\omega_o t+\phi_v^{-}-2\pi/3)\end{cases}. \quad (25)$$

Because the capacitor energy should be balanced for three phases, three Degree of Freedoms (DOFs) are needed to regulate arm energy difference, P_u^{Δ}, P_v^{Δ}, and P_w^{Δ} independently. And, the positive- and negative-sequence circulating currents provide three DOFs for arm energy balancing. Therefore, controllable positive- and negative-sequence circulating current references for balancing are defined as (26) and (27), respectively.

$$\begin{cases}i_{uo,cirAC}^{+*}=I_{cirAC}^{+}\sin(\omega_o t+\phi_i^{+})\\ i_{vs,cirAC}^{+*}=I_{cirAC}^{+}\sin(\omega_o t+\phi_i^{+}-2\pi/3)\\ i_{ws,cirAC}^{+*}=I_{cirAC}^{+}\sin(\omega_o t+\phi_i^{+}+2\pi/3)\end{cases}. \quad (26)$$

$$\begin{cases} i_{uo,cirAC}^{-*} = I_{cirAC}^{-}\sin(\omega_o t + \phi_i^{-}) \\ i_{vs,cirAC}^{-*} = I_{cirAC}^{-}\sin(\omega_o t + \phi_i^{-} + 2\pi/3) \\ i_{ws,cirAC}^{-*} = I_{cirAC}^{-}\sin(\omega_o t + \phi_i^{-} - 2\pi/3) \end{cases}. \quad (27)$$

The counterbalancing terms, $v_{xs}^{*} i_{xo,cir}$, to eliminate the difference between upper and lower arm capacitor energy are derived for three phases as (28)-(31). Eq. (28)-(31) are produced by multiplication between (24)-(25) and (26)-(27). Only DC component which plays a significant role in balancing control is presented.

$$\begin{cases} P_u^{++\Delta} = v_{us}^{+*} i_{uo,cirAC}^{+*}\big|_{DC} = \dfrac{V_{ms}^{+} I_{cirAC}^{+}}{2}\cos(\phi_v^{+} - \phi_i^{+}) \\ P_v^{++\Delta} = v_{vs}^{+*} i_{vo,cirAC}^{+*}\big|_{DC} = \dfrac{V_{ms}^{+} I_{cirAC}^{+}}{2}\cos(\phi_v^{+} - \phi_i^{+}) \\ P_w^{++\Delta} = v_{ws}^{+*} i_{wo,cirAC}^{+*}\big|_{DC} = \dfrac{V_{ms}^{+} I_{cirAC}^{+}}{2}\cos(\phi_v^{+} - \phi_i^{+}) \end{cases}. \quad (28)$$

$$\begin{cases} P_u^{+-\Delta} = v_{us}^{+*} i_{uo,cirAC}^{-*}\big|_{DC} = \dfrac{V_{ms}^{+} I_{cirAC}^{-}}{2}\cos(\phi_v^{+} - \phi_i^{-}) \\ P_v^{+-\Delta} = v_{vs}^{+*} i_{vo,cirAC}^{-*}\big|_{DC} = \dfrac{V_{ms}^{+} I_{cirAC}^{-}}{2}\cos(\phi_v^{+} - \phi_i^{-} + 2\pi/3) \\ P_w^{+-\Delta} = v_{ws}^{+*} i_{wo,cirAC}^{-*}\big|_{DC} = \dfrac{V_{ms}^{+} I_{cirAC}^{-}}{2}\cos(\phi_v^{+} - \phi_i^{-} - 2\pi/3) \end{cases}. \quad (29)$$

$$\begin{cases} P_u^{-+\Delta} = v_{us}^{-*} i_{uo,cirAC}^{+*}\big|_{DC} = \dfrac{V_{ms}^{-} I_{cirAC}^{+}}{2}\cos(\phi_v^{-} - \phi_i^{+}) \\ P_v^{-+\Delta} = v_{vs}^{-*} i_{vo,cirAC}^{+*}\big|_{DC} = \dfrac{V_{ms}^{-} I_{cirAC}^{+}}{2}\cos(\phi_v^{-} - \phi_i^{+} - 2\pi/3) \\ P_w^{-+\Delta} = v_{ws}^{-*} i_{wo,cirAC}^{+*}\big|_{DC} = \dfrac{V_{ms}^{-} I_{cirAC}^{+}}{2}\cos(\phi_v^{-} - \phi_i^{+} + 2\pi/3) \end{cases}. \quad (30)$$

$$\begin{cases} P_u^{--\Delta} = v_{us}^{-*} i_{uo,cirAC}^{-*}\big|_{DC} = \dfrac{V_{ms}^{-} I_{cirAC}^{-}}{2}\cos(\phi_v^{-} - \phi_i^{-}) \\ P_v^{--\Delta} = v_{vs}^{-*} i_{vo,cirAC}^{-*}\big|_{DC} = \dfrac{V_{ms}^{-} I_{cirAC}^{-}}{2}\cos(\phi_v^{-} - \phi_i^{-}) \\ P_w^{--\Delta} = v_{ws}^{-*} i_{wo,cirAC}^{-*}\big|_{DC} = \dfrac{V_{ms}^{-} I_{cirAC}^{-}}{2}\cos(\phi_v^{-} - \phi_i^{-}) \end{cases}. \quad (31)$$

In (28)-(31), if the positive-sequence circulating current is in phase with the output voltage, namely $\phi_v^{+} = \phi_i^{+}$, then I_{cirAC}^{+}, I_{cirAC}^{-}, ϕ_i^{-} provides three DOFs for arm energy balancing under the restriction of nullification of (21). In case of (28) and (31), because the power are equally distributed among three phases, these terms contribute to counterbalancing the upper and lower arm energy of three phases, E_{com}^{Δ}. On the other hand, in the case of (29) and (30), the differential components of the three phase arm energy difference can be eliminated, which are E_d^{Δ} and E_q^{Δ} of three phase upper and lower arm capacitor energy differences. The three power terms (P_{com}^{Δ}, P_d^{Δ}, and P_q^{Δ}) are deduced as (32)-(34).

$$\begin{aligned} P_{com}^{\Delta} &= \frac{dE_{com}^{\Delta}}{dt} = \frac{d}{dt}\{\frac{1}{3}(E_u^{\Delta} + E_v^{\Delta} + E_w^{\Delta})\} \\ &= \frac{1}{3}(P_u^{++\Delta} + P_u^{--\Delta} + P_v^{++\Delta} + P_v^{--\Delta} + P_w^{++\Delta} + P_w^{--\Delta}) \\ &= \frac{V_{ms}^{+} I_{cirAC}^{+}}{2}\cos(\phi_v^{+} - \phi_i^{+}) + \frac{V_{ms}^{-} I_{cirAC}^{-}}{2}\cos(\phi_v^{-} - \phi_i^{-}) \\ &= \frac{1}{2}(V_{ms,d}^{e+} I_{cirAC,d}^{e+} + V_{ms,q}^{e+} I_{cirAC,q}^{e+} + V_{ms,d}^{e-} I_{cirAC,d}^{e-} + V_{ms,q}^{e-} I_{cirAC,q}^{e-}). \end{aligned} \quad (32)$$

$$\begin{aligned} P_d^{\Delta} &= \frac{dE_d^{\Delta}}{dt} = \frac{d}{dt}(\frac{2}{3}E_u^{\Delta} - \frac{1}{3}E_v^{\Delta} - \frac{1}{3}E_w^{\Delta}) \\ &= \frac{2}{3}(P_u^{+-\Delta} + P_u^{-+\Delta}) - \frac{1}{3}(P_v^{+-\Delta} + P_v^{-+\Delta}) - \frac{1}{3}(P_w^{+-\Delta} + P_w^{-+\Delta}) \\ &= \frac{V_{ms}^{+} I_{cirAC}^{-}}{2}\cos(\phi_i^{-} - \phi_v^{+}) + \frac{V_{ms}^{-} I_{cirAC}^{+}}{2}\cos(\phi_v^{-} - \phi_i^{+}) \\ &= \frac{1}{2}(V_{ms,d}^{e+} I_{cirAC,d}^{e-} + V_{ms,q}^{e+} I_{cirAC,q}^{e-} + V_{ms,d}^{e-} I_{cirAC,d}^{+} + V_{ms,q}^{e-} I_{cirAC,q}^{e+}). \end{aligned} \quad (33)$$

$$\begin{aligned} P_q^{\Delta} &= \frac{dE_q^{\Delta}}{dt} = \frac{d}{dt}(\frac{\sqrt{3}}{3}E_v^{\Delta} - \frac{\sqrt{3}}{3}E_w^{\Delta}) \\ &= \frac{\sqrt{3}}{3}(P_v^{+-\Delta} + P_v^{-+\Delta}) - \frac{\sqrt{3}}{3}(P_w^{+-\Delta} + P_w^{-+\Delta}) \\ &= \frac{V_{ms}^{+} I_{cirAC}^{-}}{2}\sin(\phi_i^{-} - \phi_v^{+}) + \frac{V_{ms}^{-} I_{cirAC}^{+}}{2}\sin(\phi_v^{-} - \phi_i^{+}) \\ &= \frac{1}{2}(-V_{ms,q}^{e+} I_{cirAC,d}^{e-} + V_{ms,d}^{e+} I_{cirAC,q}^{e-} + V_{ms,q}^{e-} I_{cirAC,d}^{e+} - V_{ms,d}^{e-} I_{cirAC,q}^{e+}). \end{aligned} \quad (34)$$

For simplifying the equations, the d axis is oriented as the axis where all positive-sequence phase voltage lies ($V_{ms,q}^{e+} = 0$) and the q axis component of positive-sequence circulating current is controlled as null ($I_{cirAC,q}^{e+} = 0$) in accordance with the aforementioned synchronization of $\phi_v^{+} = \phi_i^{+}$, as (35)-(37).

$$P_{com}^{\Delta} = \frac{1}{2}(V_{ms,d}^{e+} I_{cirAC,d}^{e+} + V_{ms,d}^{e-} I_{cirAC,d}^{e-} + V_{ms,q}^{e-} I_{cirAC,q}^{e-}). \quad (35)$$

$$P_d^{\Delta} = \frac{1}{2}(V_{ms,d}^{e+} I_{cirAC,d}^{e-} + V_{ms,d}^{e-} I_{cirAC,d}^{e+}). \quad (36)$$

$$P_q^{\Delta} = \frac{1}{2}(V_{ms,d}^{e+} I_{cirAC,q}^{e-} + V_{ms,q}^{e-} I_{cirAC,d}^{e+}). \quad (37)$$

Eq. (35)-(37) can be expressed in matrix form as (38).

$$\begin{bmatrix} P_{com}^{\Delta} \\ P_d^{\Delta} \\ P_q^{\Delta} \end{bmatrix} = \frac{1}{2}\begin{bmatrix} V_{ms,d}^{e+} & V_{ms,d}^{e-} & V_{ms,q}^{e-} \\ V_{ms,d}^{e-} & V_{ms,d}^{e+} & 0 \\ V_{ms,q}^{e-} & 0 & V_{ms,d}^{e+} \end{bmatrix}\begin{bmatrix} I_{cirAC,d}^{e+} \\ I_{cirAC,d}^{e-} \\ I_{cirAC,q}^{e-} \end{bmatrix}. \quad (38)$$

Therefore, the references of the circulating current can be calculated like (39), where the determinant D is calculated as (40).

$$\begin{bmatrix} I_{cirAC,d}^{e+*} \\ I_{cirAC,d}^{e-*} \\ I_{cirAC,q}^{e-*} \end{bmatrix} = \frac{2}{D}\begin{bmatrix} (V_{ms,d}^{e+})^2 & -V_{ms,d}^{e+}V_{ms,d}^{e-} & -V_{ms,d}^{e+}V_{ms,q}^{e-} \\ -V_{ms,d}^{e+}V_{ms,d}^{e-} & (V_{ms,d}^{e+})^2 - (V_{ms,q}^{e-})^2 & V_{ms,d}^{e-}V_{ms,q}^{e-} \\ -V_{ms,d}^{e+}V_{ms,q}^{e-} & V_{ms,d}^{e-}V_{ms,q}^{e-} & (V_{ms,d}^{e+})^2 - (V_{ms,d}^{e-})^2 \end{bmatrix}\begin{bmatrix} P_{com}^{\Delta *} \\ P_d^{\Delta *} \\ P_q^{\Delta *} \end{bmatrix}. \quad (39)$$

$$D = 3V_{ms,d}^{e+}\left\{(V_{ms,d}^{e+})^2 - (V_{ms,d}^{e-})^2 - (V_{ms,q}^{e-})^2\right\}. \quad (40)$$

And then, based on (39), the proposed balancing controller can be implemented as Fig. 6.

To regulate the circulating current and produce leg voltage references, Proportional, Integral, and Resonant (PIR) controllers have been used.

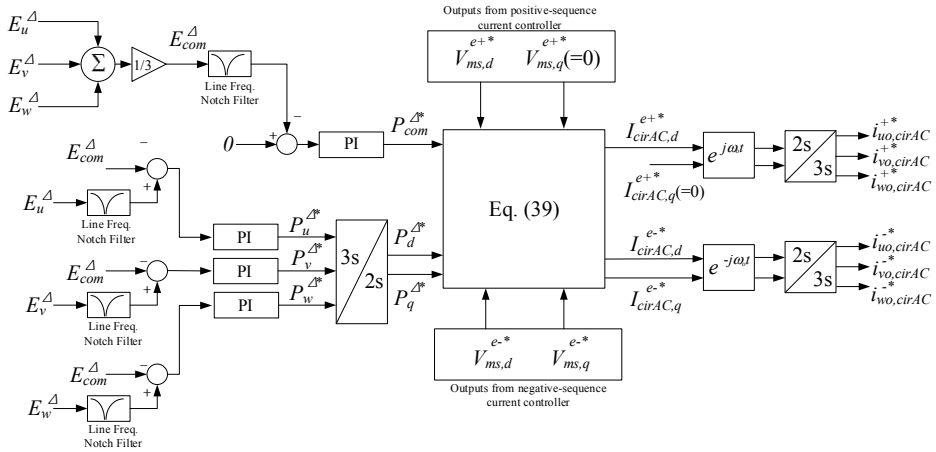

Fig. 6. Control block diagram of proposed arm energy balancing method under balanced and unbalanced grid conditions.

V. SIMULATION RESULTS

TABLE I SIMULATION PARAMETERS

Quantity	Values
Number of cells per arm	3
Rated DC bus voltage (V_{dc}^{*})	1.55kV
Rated cell capacitor voltage (V_{cell}^{*})	517V
Cell capacitor (C_{cell})	4.4mF
Grid line-to-line voltage (RMS)	550Vrms
Arm inductor inductance (L_o)	2.0 mH
Arm inductor resistance (R_o)	5.0 mΩ
DC bus R-L load inductance (L_{load})	10.0 mH
DC bus R-L load resistance (R_{load})	155 Ω
Sampling frequency (f_{samp})	8 kHz
Switching frequency (f_{sw})	4 kHz

A 4-level MMC model has been established by using time-domain simulation program, PSIM. The simulation parameters are given in Table I, referred to Fig. 1. The DC side of the MMC is connected to RL load with $L_L = 10mH$, $R_L = 150\Omega$, emulating the practical long DC transmission line.

A single line-to-ground fault is applied on AC grid at t=1.5s and lasts for 0.3s as shown in Fig 7(a). The simulations have been carried out in two cases, with and without the proposed method.

First, Fig. 7 shows dynamic performance of an MMC system with the controller described in Section IV in response to SLG fault. Fig. 7(b) shows the DC bus voltage and DC bus current. The DC bus voltage and current are sustained at the set level, even when the fault occurs. It is shown that the power flows constantly to DC line. Therefore, the magnitude of grid currents under fault condition is increased for constant power transmission, as shown in Fig. 7(c). Furthermore, the second harmonic components in DC bus voltage and current caused by negative sequence voltage are eliminated because the decoupling balancing method in [11] was applied to the

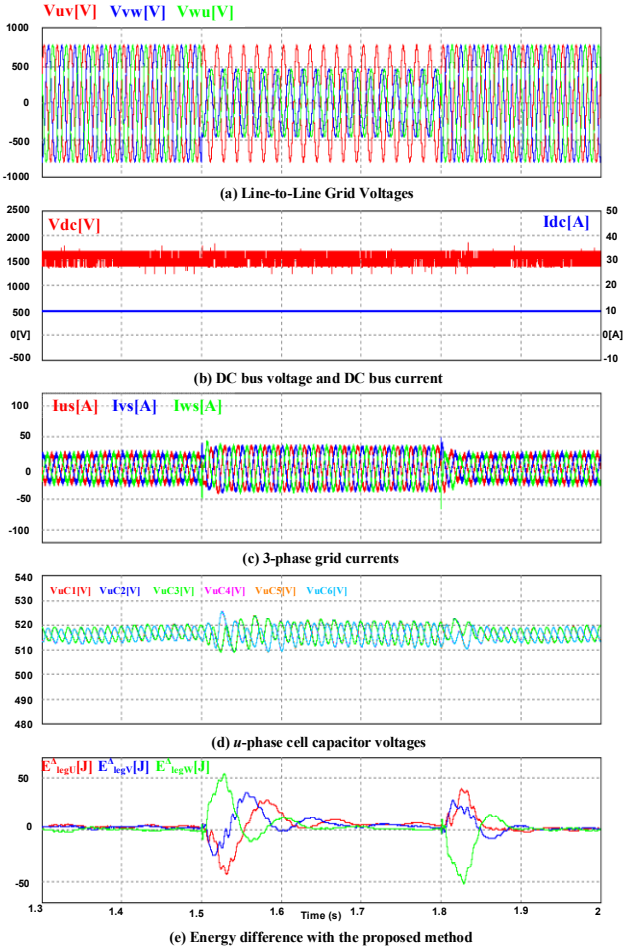

Fig. 7. Dynamic responses with the proposed control scheme under a single line-to-ground fault at grid.

proposed method basically. Fig. 7(d) shows *u*-phase cell capacitor voltages, and it can be seen that the maximum pulsation of cell capacitor voltages is around 17V (3%), which is much lower than allowable boundary. At last, energy differences between upper and lower arm capacitors at *u*, *v*, *w* leg with the proposed control scheme are shown in Fig. 7(e). From the figure, it can be seen that the energy difference are well regulated within 0.1s after SLG fault.

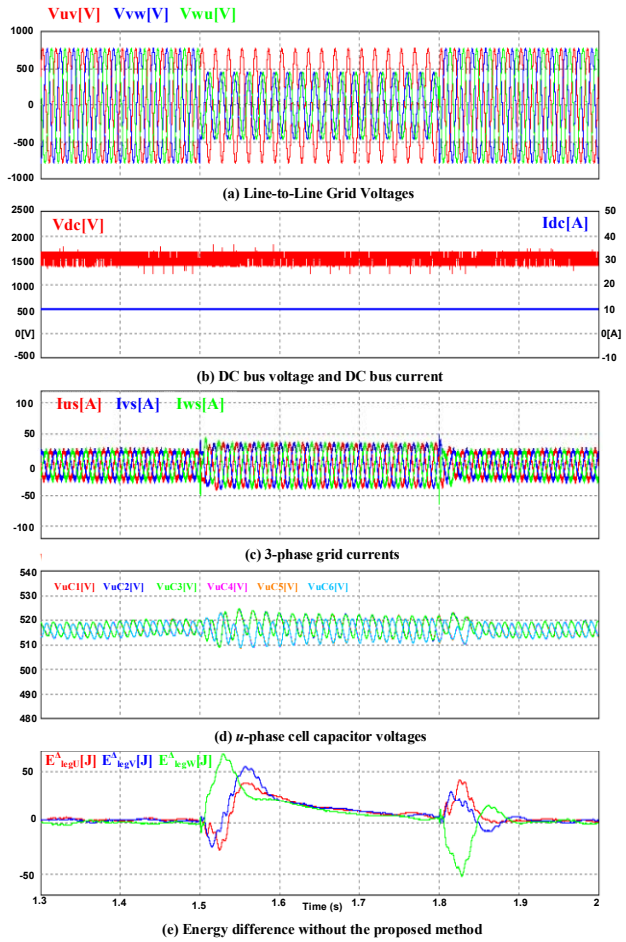

Fig. 8. Dynamic responses without the proposed control scheme under the same operating condition in Fig. 7.

In contrast, when the proposed method was not incorporated to the existing balancing controller under the same operating conditions, the energy differences between upper and lower arm capacitor are eliminated too slowly compared to that with proposed method, as shown in Fig. 8. And, the energy difference are regulated after 0.3s after SLG fault as shown in Fig. 8(e). Therefore, the proposed method could reduce the transient time by 60%.

Apart from the SLG fault conditions, to highlight the balancing performance of the proposed method, it is assumed that the negative-sequence components in grid flow into the system, although it is extreme fault situation. The magnitude of negative sequence voltage which is twice as large as positive-sequence voltage is applied on AC grid at t=1.5s, as shown in Fig. 9(a). The DC bus voltage and current, grid currents, and cell capacitor voltages fluctuate under allowable boundary because the large unbalance component in AC grid adversely affects the MMC system. However, the proposed method utilizes the negative component of output voltage for balancing, and then the upper and lower arm energy balancing is accomplished as shown in Fig. 9(e). On the other hand, the control scheme without the proposed method is also performed in simulation under the same conditions. In this case, the energy difference between upper and lower arm is considerably large and unbalanced. So, this system could not endure the same unbalance in Fig. 9(a), as shown in Fig. 10.

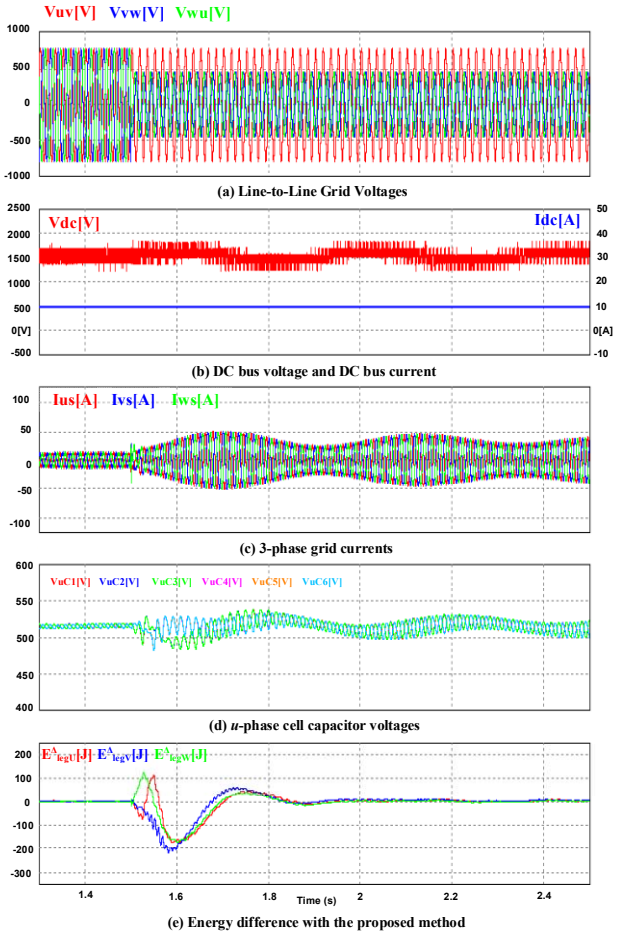

Fig. 9. Dynamic responses with the proposed control scheme under the condition that negative component is as twice as the positive component in AC grid voltage.

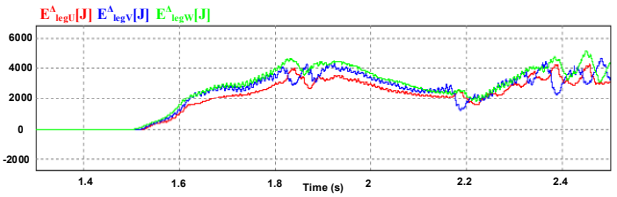

Fig. 10. Energy difference between upper and lower arm without the proposed control scheme under the same AC grid condition in Fig. 9.

VI. CONCLUSIONS

A control strategy of the MMC for capacitor energy balancing has been presented, which is universally valid under both balanced and unbalanced grid condition without any transition in control modes. By exploiting the inevitable negative-sequence component in output phase voltage for capacitor balancing, the dynamics of cell voltage balancing have been improved under asymmetric

fault conditions.

The simulation study in this paper mainly focused on the dynamic response of the proposed method under the single line-to-ground terminal bus fault. The validity of the proposed method has been supported by computer simulation results. The fault ride-through capability of the MMC could be much enhanced if the proposed control method is incorporated in the existing cell voltage balancing controller.

REFERENCES

[1] S. Allebrod, R. Hamerski, and R. Marquardt, "New transformerless, scalable modular multilevel converters for HVDC-transmission," in *Proc. IEEE PESC*, 2008, pp. 174-179.

[2] A. Lesnicar and R. Marquardt, "An innovative modular multilevel converter topology suitable for a wide power range," in *Proc. IEEE Boogna Power Tech*, 2008, vol. 3, pp. 1-6.

[3] D. Peftitsis, G. Tolstoy, A. Antonopoulos, J. Rabkowski, J. K. Lim, M. Bakowski, L. Angquist, and H. P. Nee, "High-power modular multilevel converters with SiC JFETs," in *Proc. IEEE ECCE*, 2010, pp. 2148-2155.

[4] AmirnaserYazdani, and Reza Iravani, "Voltage-Sourced Converters in Power Systems –Modeling, Control, and Applications," *IEEE Press*, 2011.

[5] Soto-Sanchez, D.; Green, T.C., "Control of a modular multilevel converter-based HVDC transmission system," *Power Electronics and Applications (EPE 2011), Proceedings of the 2011-14th European Conference on* , vol., no., pp.1,10, Aug. 30 2011-Sept. 1 2011.

[6] X. Chen, C. Zhao, C. Cao, "Research on the fault characteristics of HVDC based on modular multilevel converter," Electrical Power and Energy Conference (EPEC), 2011 IEEE, pp.91,96, 3-5 Oct. 2011.

[7] Bordignon, P.; Marchesoni, M.; Parodi, G.; Vaccaro, L. "Modular multilevel converter in HVDC systems under fault conditions", Power Electronics and Applications (EPE), 2013 15th European Conference on, On page(s): 1 – 10

[8] Minyuan Guan; Zheng Xu, "Modeling and Control of a Modular Multilevel Converter-Based HVDC System Under Unbalanced Grid Conditions," *Power Electronics, IEEE Transactions on* , vol.27, no.12, pp.4858,4867, Dec. 2012.

[9] Qingrui Tu; Zheng Xu; Yong Chang; Li Guan, "Suppressing DC Voltage Ripples of MMC-HVDC Under Unbalanced Grid Conditions," *Power Delivery, IEEE Transactions on* , vol.27, no.3, pp.1332,1338, July 2012.

[10] Yazdani, A.; Iravani, R., "A unified dynamic model and control for the voltage-sourced converter under unbalanced grid conditions," *Power Delivery, IEEE Transactions on* , vol.21, no.3, pp.1620,1629, July 2006.

[11] S.H. Choi, S. Kim, J. J. Jung, and S. K. Sul, "A Comprehensive Cell Capacitor Energy Control Strategy of a Modular Multilevel Converter (MMC) without a Stiff DC Bus Voltage Source," *2014 Applied Power Electronics Conference and Exposition*, 2014-Mar., 2014.

[12] Jae-Jung Jung, Hak-Jun Lee, and Seung-Ki Sul, "Control strategy for improved dynamic performance of variable-speed drives with the Modular Multilevel Converter," in *IEEE Energy Conversion Congress and Exposition*, pp. 1481-1488, 2013.